Available online at www.sciencedirect.com

ScienceDirect

Spectrochimica Acta Part A 66 (2007) 236–242

SPECTROCHIMICA ACTA PART A

www.elsevier.com/locate/saa

Photophysical properties of novel lanthanide (Tb^{3+}, Dy^{3+}, Eu^{3+}) complexes with long chain *para*-carboxyphenol ester *p*-L-benzoate (L = dodecanoyloxy, myristoyloxy, palmitoyloxy and stearoyloxy)

Bing Xu, Bing Yan [*]

Department of Chemistry, Tongji University, Shanghai 200092, PR China

Received 30 November 2005; accepted 22 February 2006

Abstract

In this paper, a series of 12 binary luminescent lanthanide coordination compounds with long chain *p*-carboxyphenol ester were assembled. Both elemental analysis and infrared spectroscopy allowed to determine the complexes formula: LnL_3, where Ln = Tb, Dy, Eu; L = *p*-dodecanoyloxybenzoate (12-OBA), *p*-myristoyloxybenzoate (14-OBA), *p*-palmitoyloxybenzoate (16-OBA) and *p*-stearoyloxybenzoate (18-OBA), respectively. The photophysical properties of these complexes were studied in detail with various of spectroscopies such as ultraviolet–visible absorption spectra, low temperature phosphorescence spectra and fluorescent spectra. The ultraviolet–visible absorption spectra showed that some bands shift with the different chain length of *p*-carboxyphenol ester. From the low temperature phosphorescent emission, the triplet state energies for these four ligands were determined to be around 24,242 cm^{-1} (12-OBA), 24,612 cm^{-1} (14-OBA), 24,084 cm^{-1} (16-OBA) and 24,125 cm^{-1} (18-OBA), respectively, suggesting they are suitable for the sensitization of the above lanthanide ions, especially for Tb^{3+} and Dy^{3+}. The fluorescence excitation and emission spectra for these lanthanide complexes of the four ligands take agreement with the above predict from energy match.

Keywords: Lanthanide complexes; Long chain *p*-carboxyphenol ester; Photophysical property; Energy transfer; Spectroscopy

1. Introduction

The study of the trivalent rare earth ions (RE^{3+}) complexes continues to be an active research area, which may be attributed to the luminescent properties of these compounds and their applications as optical signal amplifiers, electroluminescent devices and luminescent probes or labels in biological systems [1–4]. Considerable studies have been focused on the design and assembly of lanthanide complexes with organic ligands such as aromatic carboxylic acids, β-diketones, cryptands, calixarenes, heterocyclic ligands, etc. [5–8]. In fact, the photophysical properties of lanthanide compounds markedly depend on their environment. Unless very intense irradiation is used for direct excitation of the weak lanthanide f–f transitions, emission has to be sensitized by energy transfer from a suitable adjacent chromophore. To get an efficient cation emission, the antenna intersystem crossing quantum yield, the antenna-lanthanide distance and the overlap between the energy levers of donor and acceptor are the three main factors, in which the energy transfer – usually an organic chromophore – plays an essential role. Only when organic chromophore absorbs light strongly in the UV region to overcome the difficulty of direct excitation into the parity then transfers it to the lanthanide ion efficiently, and at the same time protects central cation from solvent molecules that can quench the central metal emission can it be selected. Therefore, the encapsulation of the lanthanide ion in an organic ligand has been become fascinating areas of research, because it improves not only the processibility of lanthanide ions in organic matrices but also its optical properties, as the ligand shields the lanthanide ion from its environment. For binary complexes, it was found that most β-diketone derivatives are more suitable for luminescence of Eu^{3+} [9–13] while most aromatic carboxylic acids are more suitable for the luminescence of Tb^{3+} [14–18]. We also have studied the energy match and intramolecular energy transfer mechanism in ternary lanthanide complexes with aromatic carboxylic acids and 1,10-phenanthroline in details

---

[*] Corresponding author. Tel.: +86 21 65984663; fax: +86 21 65982287.
E-mail address: byan@tongji.edu.cn (B. Yan).

1386-1425/$ – see front matter © 2006 Elsevier B.V. All rights reserved.
doi:10.1016/j.saa.2006.02.047

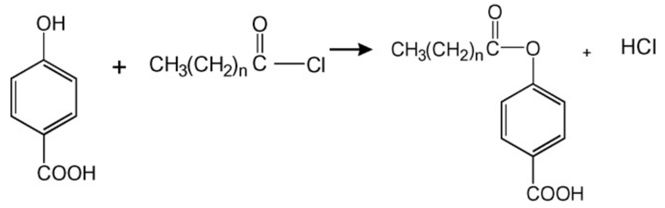

Scheme 1. Synthesis of long chain phenol ester by modification of *para*-hydroxybenzoic acid with L-chloride (L = 1-dodecanoyl, 1-myristoyl, 1-palmitoyl and 1-stearoyl) (n = 10, 12, 14, 16).

[19,20], indicating there still exist intramolecular energy transfer mechanism between ligands (i.e. from aromatic carboxylic acids and 1,10-phenanthroline). On account of the energy match and energy transfer mechanism, it can be realized to predict the luminescent properties of lanthanide complexes. Phthalate and aminobenzoate derivative have been found to exhibit favorable properties of luminescence and film formation [21,22], but the hydroxybenzoate derivatives has not been investigated.

In this context, using *para*-hydroxybenzoic acid as original material, four kinds of long chain *p*-carboxyphenol ester were achieved, i.e. *p*-dodecanoyloxybenzoate (12-OBA), *p*-myristoyloxybenzoate (14-OBA), *p*-palmitoyloxybenzoate (16-OBA) and *p*-stearoyloxybenzoate (18-OBA), respectively. The corresponding lanthanide (Tb^{3+}, Dy^{3+} and Eu^{3+}) complexes with these ligands were synthesized and characterized. The photophysical properties for these long carboxyphenol ester and their lanthanide complexes were studied in detail, which can be expected to have practical application to fabricate the Langmuir-Blodgett films.

2. Experimental

2.1. Synthesis of p-carboxyphenol ester by the modification of p-hydroxybenzoic acid

Para-hydroxybenzoic acid (1.37 g) was dissolved into acetone, equimolar amount of long chain L-chloride (1-dodecanoyl chloride (2.18 g), 1-myristoyl chloride (2.46 g), 1-palmitoyl chloride (2.74 g) and 1-stearoyl chloride (3.03 g)) was added into the acetone solution slowly. Then the mixture was placed in a water bath at the temperature 65–70 °C and react for 10 h. Finally the samples were recrystallized with ethanol three times to afford the products (Scheme 1). The compositions of the aim products were confirmed by elemental analysis: Calcd. for $C_{19}H_{28}O_4$: C, 71.25; H, 8.75; Found: C, 71.65; H, 9.00. H NMR δ 7.98 (2H), 7.25 (2H), 3.74 (2H), 2.34 (2H), 1.63 (2H), 1.27 (14H), 0.88 (3H), 10.50 (–COOH). For $C_{21}H_{32}O_4$: C, 72.41; H, 9.20; Found: C, 72.95; H, 9.59. H NMR δ 7.98 (2H), 7.37 (2H), 3.88 (2H), 2.34 (2H), 1.72 (2H), 1.25 (18H), 0.89 (3H), 10.62 (–COOH). For $C_{23}H_{36}O_4$: C, 73.40; H, 9.57; Found: C, 73.61; H, 9.85. H NMR δ 8.01 (2H), 7.59 (2H), 4.12 (2H), 2.15 (2H), 1.27 (24H), 0.88 (3H), 10.50 (–COOH). For $C_{25}H_{40}O_4$: C, 74.26; H, 9.90; Found: C, 74.61; H, 10.01. H NMR δ 7.97 (2H), 7.55 (2H), 3.54 (2H), 3.01 (2H), 1.38 (28H), 0.87 (3H), 10.59 (–COOH).

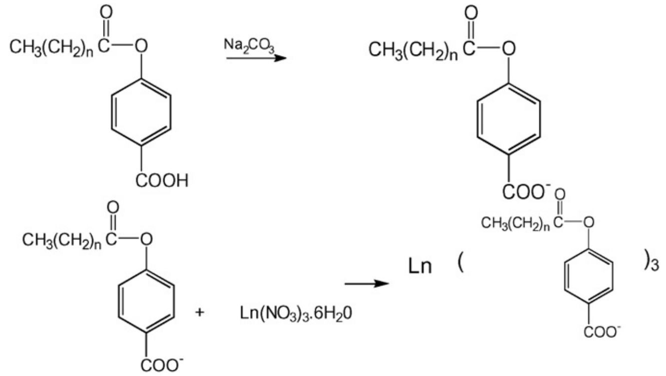

Scheme 2. Synthesis of lanthanide complexes with long chain carboxyphenol ester (Ln = Eu, Tb, Dy; n = 10, 12, 14, 16).

2.2. Synthesis of lanthanide complexes with long chain p-carboxyphenol ester

The lanthanide oxides (Eu_2O_3, Tb_4O_7 and Dy_2O_3) were converted to their nitrates by treatment with concentrated nitric acid. *p*-L-oxybenzoic acid (0.318 g for 12-OBA, 0.344 g for 14-OBA, 0.374 g for 16-OBA and 0.403 g for 18-OBA; 1.0 mmol) was dissolved into the aqueous solution of Na_2CO_3 (0.1 mol L^{-1}). Then aqueous solution of lanthanide nitrate ($Ln(NO_3)_3\cdot 6H_2O$, L = Eu, Tb, Dy; 0.33 mmol) was added very slowly to above mixed solution with vigorous stirring, resulting in white solid products (Scheme 2). After stirring for 1 h, the product was filtered, washed with ethanol and water repeatedly and dried in desiccator. The compositions of the complexes were confirmed by elemental analysis: $Ln(L)_3$, Ln = Eu, Tb, Dy; L = 12-OBA, 14-OBA, 16-OBA and 18-OBA. Anal. Calcd. for $C_{57}H_{84}O_{12}Eu$: C, 61.68; H, 7.57; Found: C, 61.92; H, 7.16. For $C_{63}H_{93}O_{12}Eu$: C, 63.37; H, 7.80; Found: C, 63.07; H, 7.42. For $C_{69}H_{105}O_{12}Eu$: C, 64.84; H, 8.22; Found: C, 65.21; H, 7.89. For $C_{75}H_{117}O_{12}Eu$: C, 66.13; H, 8.60; Found: C, 66.40; H, 8.18. For $C_{57}H_{84}O_{12}Tb$: C, 61.29; H, 7.26; Found: C, 61.03; H, 7.01. For $C_{63}H_{93}O_{12}Tb$: C, 63.00; H, 7.75; Found: C, 63.26; H, 7.44. For $C_{69}H_{105}O_{12}Tb$: C, 64.48; H, 8.18; Found: C, 64.19; H, 7.93. For $C_{75}H_{117}O_{12}Tb$: C, 65.79; H, 8.55; Found: C, 65.97; H, 8.20. For $C_{57}H_{84}O_{12}Dy$: C, 61.10; H, 7.50; Found: C, 61.40; H, 7.12. For $C_{63}H_{93}O_{12}Dy$: C, 62.82; H, 7.73; Found: C, 63.14; H, 7.47. For $C_{69}H_{105}O_{12}Dy$: C, 64.31; H, 8.16; Found: C, 64.60; H, 7.88. For $C_{75}H_{117}O_{12}Dy$: C, 65.62; H, 8.53; Found: C, 65.35; H, 8.23.

2.3. Physical measurements

Elemental analyses (C, H) were carried out by the Elementar Cario EL elemental analyzer. Infrared spectroscopy with KBr pellets was performed on a Nicolet Nexus 912 AO446 model spectrophotometer in the 4000–400 cm^{-1}. Ultraviolet absorption spectra were obtained with an Agilent 8453 spectrophotometer. Low temperature phosphorescence spectrum was determined Perkin-Elmer LS-55 spectrophotometer at 77 K. The fluorescence (excitation and emission) spectra were determined with Perkin-Elmer LS-55 spectrophotometer: excitation slit width = 10 nm, emission slit width = 5 nm.

3. Results and discussion

All the IR spectra of these lanthanide complexes show the similar features. For example, in the IR spectra of Ln(12-OBA)$_3$ system, the characteristic absorption peaks of the carboxylic group appear at 1548, 1548, 1548 cm^{-1} for ν_{as} (COO–) and 1442, 1442, 1466 for ν_s (COO–), respectively, while there does not exist for free 12-OBA ligand, suggesting that the oxygen atoms of 12-OBA carbonyl group are coordinated with Ln^{3+}. The characteristic absorption band of the carbonyl group shifts from high wave number of 1702.45 cm^{-1} for 12-OBA to a lower value of 1671.75 cm^{-1} for Ln(12-OBA)$_3$ and the absorption intensity is weaker for complexes than that of 12-OBA, suggesting there still exist one carboxyl group in the long chain carboxyphenol ester and these carbonyl groups coordinated with Ln ions. For the IR spectra of Ln(14-OBA)$_3$ system, the characteristic absorption peaks of the carboxylic group emerge at 1548, 1544, 1552 cm^{-1} for ν_{as} (COO–) and 1470, 1433, 1470 cm^{-1} for ν_s (COO–), respectively, while it is not observed in the spectra of free 14-OBA ligand, indicating that the oxygen atoms of 14-OBA carbonyl group are coordinated with Ln^{3+}. Both the free ligand and its complexes show the characteristic absorption bands of carbonyl group (1703.52 cm^{-1} (s) for 14-OBA and 1671.79 cm^{-1} for Ln(14-OBA)$_3$) except for the weaker absorption intensity for complexes than that of 14-OBA, which indicates that there still exist one carbonyl group in the long chain carboxyphenol ester which also take part in coordination with Ln ions. In the IR spectra of Ln(16-OBA)$_3$ system, the characteristic absorption peaks of the carboxylic group are shown at 1552, 1531, 1552 cm^{-1} for ν_{as} (COO–) and 1470, 1470, 1470 cm^{-1} for ν_s (COO–), respectively, while they are not present for free 16-OBA ligand, which illuminates that the oxygen atoms of mono 16-OBA carbonyl group are coordinated with Ln^{3+}. The free ligand and its complexes show the characteristic absorption bands of the carbonyl group at 1704.42 cm^{-1} (strong) and 1744.38 cm^{-1}, respectively, and the intensity of the latter is much weaker than that of complexes, verifying that there still exists one carboxyl group of long chain carboxyphenol ester. In the IR spectra of Ln(18-OBA)$_3$ system, the characteristic absorption peaks of the carboxylic group are located at 1544, 1527, 1548 cm^{-1} for ν_{as} (COO–) and 1413, 1380, 1413 cm^{-1} for ν_s (COO–), respectively. While these peaks are not present for free 18-OBA ligand, which indicate that the oxygen atoms of mono 18-OBA carbonyl group are coordinated with Ln^{3+}. The characteristic absorption bands of the carbonyl group for complexes (1671.74 cm^{-1}) show blue shift compared with their corresponding ligand (1705.54 cm^{-1}, strong), suggesting that there still exist one carboxyl group of long chain carboxyphenol ester which also coordinate with lanthanide ions (Table 1).

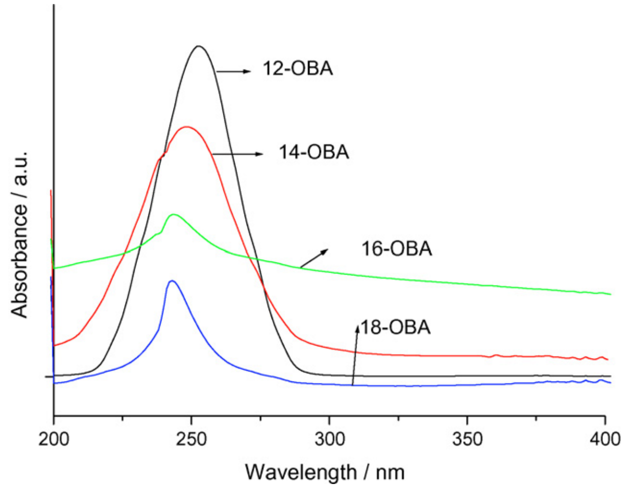

Fig. 1. Ultraviolet–visible absorption spectra of long chain carboxyphenol esters.

Fig. 1 shows the representative ultraviolet–visible absorption spectra for the four long chain ligands (12-OBA, 14-OBA, 16-OBA and 18-OBA). They all exhibit domain absorption peaks in the ultraviolet region of 200–400 nm, and the maximum absorption peaks are located at 252 nm (12-OBA), 248 nm (14-OBA), 244 nm (16-OBA) and 243 nm (18-OBA), respectively, which

Table 1
The IR spectra data and band assignments of the lanthanide complexes

Complex	$\nu_{s\,CH_3}$	$\nu_{as\,CH_3}$	$\nu_{C{=}O}$	$\nu_{s\,COO-}$	$\nu_{as\,COO-}$	$\nu_{s\,C-O-C}$	$\nu_{as\,C-O-C}$
12-OBA	2847.67	2917.14	1702.45			1111.01	1249.94
Dy-12-OBA	2847.67	2917.14	1671.75	1548.24	1442.00	1111.01	1239.64
Eu-12-OBA	2847.67	2917.14	1671.75	1548.24	1442.00	1111.01	1239.64
Tb-12-OBA	2851.76	2917.14	1671.75	1548.24	1466.52	1111.01	1239.64
14-OBA	2847.67	2917.14	1703.52			1172.60	1286.72
Dy-14-OBA	2847.67	2917.14	1671.79	1548.24	1470.60	1106.92	1284.72
Eu-14-OBA	2847.67	2917.14	1671.79	1544.15	1433.83	1106.92	1284.72
Tb-14-OBA	2848.67	2921.23	1671.79	1552.33	1470.60	1111.01	1284.72
16-OBA	2847.67	2917.14	1704.42			1098.75	1298.98
Dy-16-OBA	2847.67	2921.23	1744.38	1552.33	1470.60	1111.01	1287.38
Eu-16-OBA	2847.67	2921.2	1744.38	1531.90	1470.60	1115.10	1287.38
Tb-16-OBA	2847.67	2917.14	1744.38	1552.33	1470.60	1111.01	1287.38
18-OBA	2851.89	2916.76	1705.54			1074.59	1288.65
Dy-18-OBA	2851.76	2917.14	1671.74	1544.15	1413.39	1106.92	1285.65
Eu-18-OBA	2843.59	2917.14	1671.74	1527.81	1380.70	1111.01	1285.65
Tb-18-OBA	2847.67	2917.14	1671.74	1548.24	1413.39	1111.01	1285.65

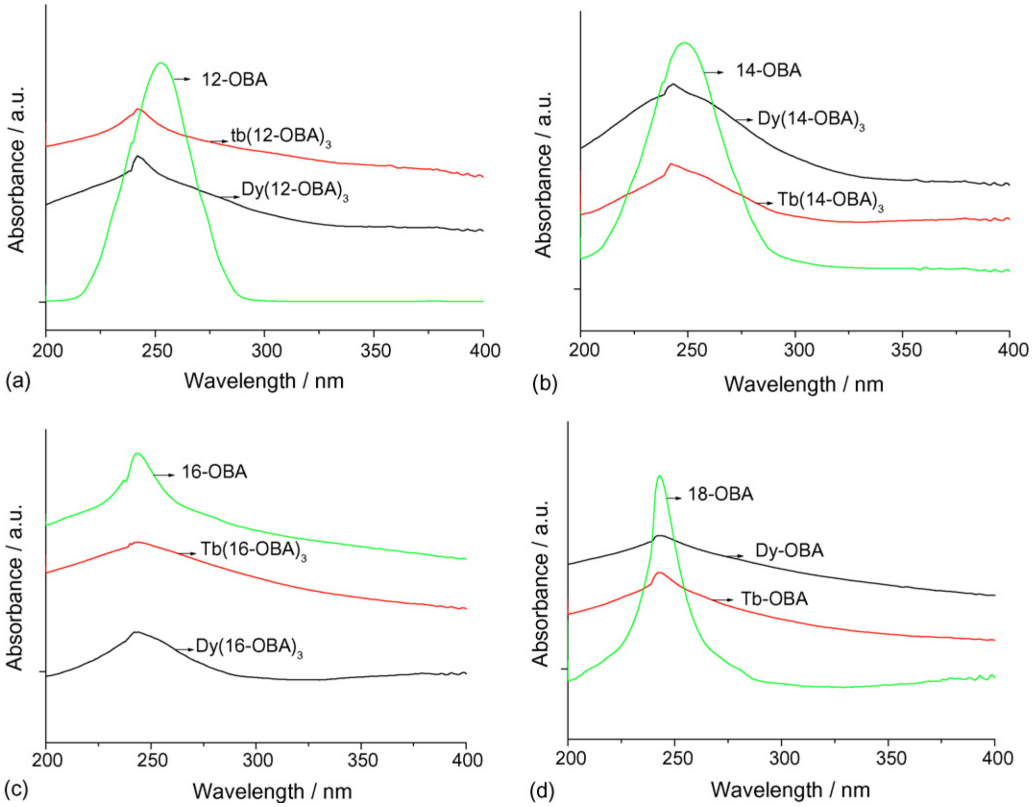

Fig. 2. Ultraviolet–visible absorption spectra of long chain carboxyphenol and its lanthanide complexes: (a) 12-OBA and Ln(12-OBA)$_3$; (b) 14-OBA and Ln(14-OBA)$_3$; (c) 16-OBA and Ln(16-OBA)$_3$; (d) 18-OBA and Ln(18-OBA)$_3$.

are ascribed to the characteristic absorption peaks of phenyl ring with long chain substituted groups. The little distinction of band position and intensity is due to the different chain length (12-OBA-14OBA-16OBA-18OBA). Besides, it can be observed that the maximum absorption bands exhibit small blue shifts with the increase of chain length, suggesting the increase of substituted chain length influences the electron distribution in along the phenyl ring. Fig. 2(a–d) exhibits the absorption spectra of Ln-12-OBA, Ln-14-OBA, Ln-16-OBA and Ln-18-OBA (Ln = Tb, Dy), respectively. All of them show blue shifts compared with the corresponding free ligands: 242 nm for Ln-12-OBA, 242.5 nm for Ln-14-OBA, 242 nm for Ln-16-OBA and 241 nm for Ln-18-OBA separately, it is estimated that during the process of complexation, lanthanide ions may hinder the conjugating effect of double bonds (C=C and C=O) and enlarge the energy difference levels among the electron transitions.

We further measured the low temperature phosphorescence spectra of the four long chain ligands at 77 K. From the maximum phosphorescent emission band (412.5 nm for 12-OBA, 406 nm for 14-OBA, 415 nm for 16-OBA and 414.5 nm for 18-OBA, respectively), the triplet state energies can be determined as 24,242 cm^{-1} (12-OBA), 24,612 cm^{-1} (14-OBA), 24,084 cm^{-1} (16-OBA) and 24,125 cm^{-1} (18-OBA), separately. The energy differences between the triplet state of the four ligands (12-OBA, 14-OBA, 16-OBA and 18-OBA) and the resonance energy levels of Eu^{3+} ($^5D_0$, 17,265 cm^{-1}), Tb^{3+} ($^5D_4$, 20,500 cm^{-1}) and Dy^{3+} ($^4F_{9/2}$, 21,000 cm^{-1}) can be calculated and the detailed data have been shown in Table 2. According to the intramolecular energy mechanism [23–26], the intramolecular energy transfer efficiency depends chiefly on two energy transfer processes: the first one leads from the triplet level of ligands to the emissive energy level of the Ln^{3+} ion by Dexter's resonant exchange interaction [27]; the second one is just an inverse energy transfer by a thermal deactivation mechanism. Both energy transfer rate constants depend on the energy differences between the triplet level of the ligands and the resonant emissive energy of Ln^{3+}. Intramolecular energy transfer efficiency in lanthanide complexes conforms to Dexter's exchange energy transfer theory [27]:

$$K_{\mathrm{ET}} = \left(\frac{2\pi Z^2}{R}\right) \exp\left(\frac{r}{l}\right) \int F_{\mathrm{d}}(E) F_{\mathrm{a}}(E)\,\mathrm{d}E \qquad (1)$$

where K_{ET} is the rate constant of energy transfer, r the intermolecular distance between the energy donor and acceptor atoms, l the van der Waals radius, the integral represents the

Table 2
The phosphorescence spectra data of aromatic carboxylic acids

Ligands	Triplet state energies (cm^{-1})	ΔE(Tr-Eu^{3+}) (cm^{-1})	ΔE(Tr-Tb^{3+}) (cm^{-1})	ΔE(Tr-Dy^{3+}) (cm^{-1})
12-OBA	24242	6977	3742	3242
14-OBA	24612	7347	4112	3612
16-OBA	24084	6819	3584	3084
18-OBA	24125	6860	3625	3125

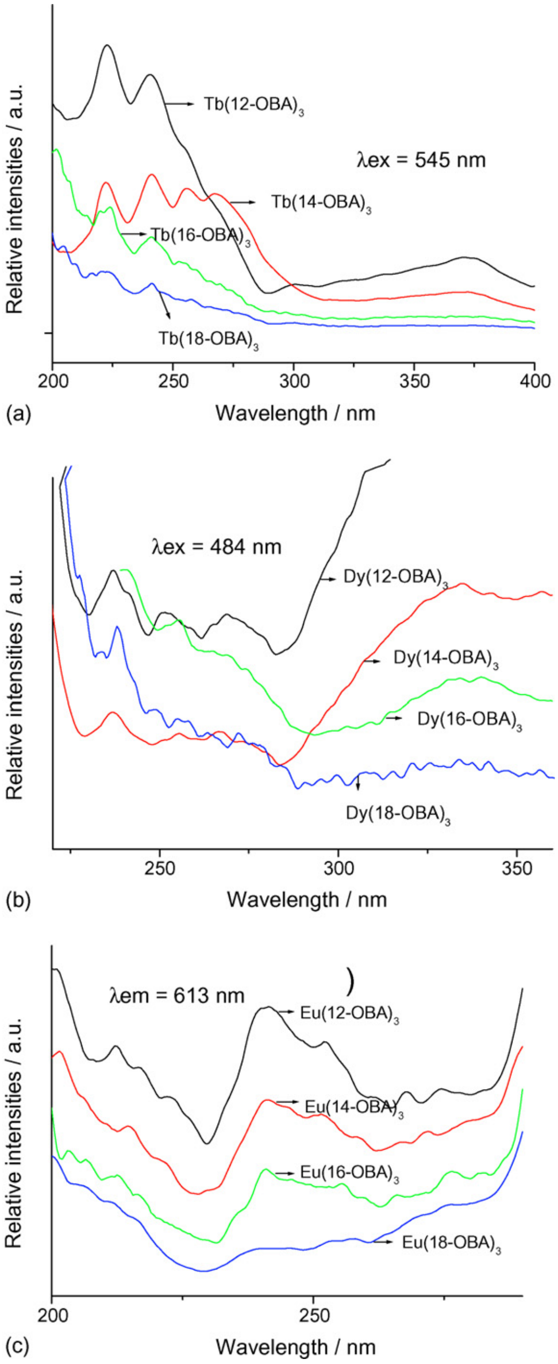

Fig. 3. Excitation spectra of lanthanide complexes with long chain carboxyphenol ester: (a) $Tb(L)_3$, (b) $Dy(L)_3$ and (c) $Eu(L)_3$ (L = 12-OBA, 14-OBA, 16-OBA and 18-OBA).

overlap between the luminescence spectrum of the ligands and the absorption spectrum of Ln^{3+} ($F_d(E)$: the luminescence spectrum of energy donor (ligand), $F_a(E)$: absorption spectrum of energy acceptor (Ln^{3+})), and $2\pi Z^2/R$ is a constant relating to the mutual distance between Ln^{3+} and coordinated atom. r and l are both considered to be constant for intramolecular energy transfer processes. From Eq. (1), K_{ET} increases with decreasing energy difference ΔE(Tr-Ln^{3+}) between the triplet state energy of ligands and the resonance emission energy of Eu^{3+} and Tb^{3+}. Thus, ligands with a large energy difference cannot sensitize rare earth ions effectively. On the other hand, there exists an inverse energy transfer process which affects luminescence intensity by temperature ($k(T)$ [28]: rate constant of inverse energy transfer process (thermal deactivation process), A: pre-exponential factor):

$$k(T) = A\ \exp\left(-\frac{\Delta E(\text{Tr-Ln}^{3+})}{RT}\right) \tag{2}$$

It can be seen that the activation energy is approximately equal to ΔE(Tr-Ln^{3+}) in the inverse energy transfer process; therefore, a decreasing energy difference increases $k(T)$. Based on this evidence, the conclusion can be drawn that ΔE(Tr-Ln^{3+}) is of opposite influence on the two energy transfer processes and an optimal value can be assumed to exist (around $3000 \pm 500\,\text{cm}^{-1}$). From the data in Table 2, it can be primarily predicted that the energy transfer process will occur from the long ligands to the three Ln ions, especially for Tb^{3+} and Dy^{3+}.

Fig. 3(a–c) gives the excitation spectra of Tb, Dy and Eu solid complexes with the four ligands. The excitation bands for Tb complexes under the green emission of 545 nm mainly take place in the narrow range from 210 to 300 nm and some apparent peaks are shown: 223 and 241 nm for Tb-12-OBA, 222, 241, 256 and 267 nm for Tb-14-OBA, 223 and 241 nm for Tb-16-OBA and 222, 241 and 257 nm for Tb-18-OBA. Under the blue emission of 484 nm, the excitation bands for Dy complexes exhibit obvious peaks: 237, 255, 269 and 339 nm for Dy-12-OBA, 237, 256 and 267 nm for Dy-14-OBA, 241, 255 and 333 nm for Dy-16-OBA and 237 and 255 nm for Dy-18-OBA. The excitation bands for Eu complexes under the red emission of 613 nm show broad excitation bands and the maximum excitation peaks are located around 241 nm for Eu-12-OBA, 241 nm for Eu-14-OBA and 241 nm for Eu-16-OBA, respectively. The excitation spectrum of Eu-18-OBA shows some differences from the above three Eu complexes, which exhibit three apparent peaks at 241, 255 and 276 nm. We further measured the corresponding emission spectra by selective excitation with the different excitation wavelengths, they show the similar emission position except for different luminescent intensities.

Figs. 4–6 show the selected emission spectra of Tb, Dy and Eu complexes with these four ligands. For Tb complexes, all of which exhibit similar behavior. The emission spectra under the excitation of 241 nm show two apparent emission peaks at 489 and 544 nm attributed to be the characteristic emission $^5D_4 \rightarrow {}^7F_J$ (J = 6, 5) transition of Tb^{3+} ion, indicating that the four long ligands are good sensitizers for the Tb^{3+} luminescence. Among the $^5D_4 \rightarrow {}^7F_5$ transition exhibits the strongest green emission. For Dy complexes, two apparent emission peaks under the excitation of 256 nm are observed: one is at 482 nm for Dy-12-OBA, 482 nm for Dy-14-OBA, 484.5 nm for Dy-16-OBA and 483.5 nm for Dy-18-OBA; the other is at 578 nm for Dy-12-OBA, 579 nm for Dy-14-OBA, 575 nm for Dy-16-OBA and 574.5 nm for Dy-18-OBA separately, which correspond to the characteristic $^4F_{9/2} \rightarrow {}^6H_J$ (J = 15/2, 13/2) transition of Dy^{3+} ion, suggesting that the energy transition goes smoothly from triplet state of the four ligands to emissive energy level of

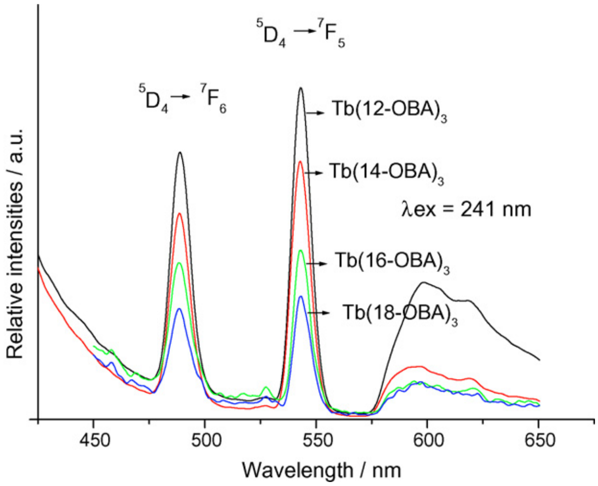

Fig. 4. Emission spectra of Tb complexes with long chain carboxyphenol ester.

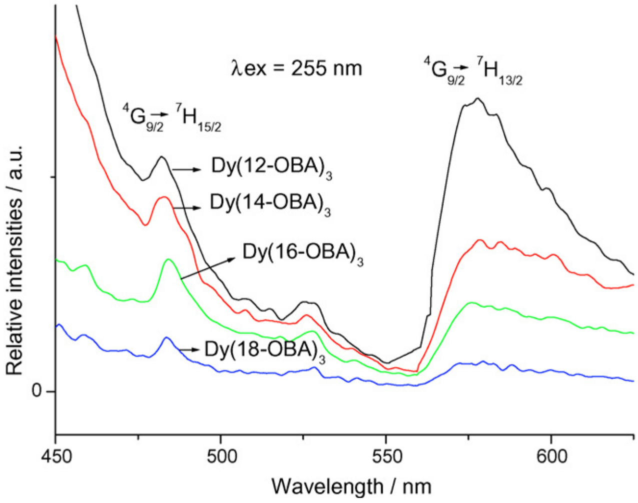

Fig. 5. Emission spectra of Dy complexes with long chain carboxyphenol ester.

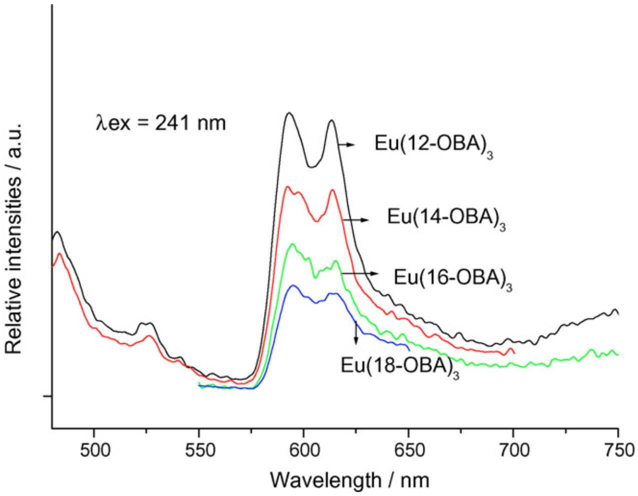

Fig. 6. Emission spectra of Eu complexes with long chain carboxyphenol ester.

Dy^{3+} ion. For europium complexes, the spectrum for europium complexes were not ideal, two peaks of the emission spectra corresponding to the emissions originated from $^5D_0 \rightarrow {}^7F_J$ transitions ($J = 1$, 2) of Eu^{3+} ion have not been divided absolutely and they are located at 593, 593, 594, 596 nm and 613, 613, 615, 614 nm for Eu-12-OBA, Eu-14-OBA, Eu-16-OBA and Eu-18-OBA separately. The overlap of the two transitions suggests that the long chain carboxyphenol ester is not suitable for the sensitization of the Eu^{3+} ion, which has a good agreement with the data from Table 2.

4. Conclusions

Four long chain carboxyphenol ester ligands have been synthesized and their 12 complexes with lanthanide ions (Tb^{3+}, Dy^{3+} and Eu^{3+}) have been prepared. The photophysical properties of them have been studied with ultraviolet spectra, low temperature phosphorescent spectra, excitation and emission spectra. The triplet state energy of the four long chain ligands are determined to be 24,242 cm^{-1} (12-OBA), 24,612 cm^{-1} (14-OBA), 24,084 cm^{-1} (16-OBA) and 24,125 cm^{-1} (18-OBA), respectively, with the phosphorescence spectra. The energy match between the long chain ligands and lanthanide ions (Tb^{3+}, Dy^{3+} and Eu^{3+}) has been studied to predict that the optimum energy transfer exists between the ligand and Ln^{3+}.

Acknowledgement

This work was supported by the National Natural Science Foundation of China (20301013).

References

[1] Y.X. Ci, Y.Z. Li, W.B. Chang, Anal. Chim. Acta 248 (1991) 589.
[2] L.K. Scott, W.D. Horrocks, J. Inorg. Biochem. 46 (1992) 193.
[3] J. Kido, Y. Okamoto, Chem. Rev. 102 (2002) 2357.
[4] R. Reyes, E.N. Hering, M. Cremona, C.F.B. Silva, H.F. Brito, C.A. Achete, Thin Solid Films 23 (2002) 420.
[5] Y.S. Yang, M.L. Gong, Y.Y. Li, H.Y. Lei, S.L. Wu, J. Alloys Compd. 207/208 (1994) 112.
[6] C.J. Feng, Q.H. Luo, C.Y. Duan, J. Chem. Soc., Dalton Trans. (1998) 377.
[7] T. Gunnlaugsson, A.J. Harte, J.P. Leonard, M. Nieuwenhuyzen, Chem. Commun. (2002) 2135.
[8] B. Yan, Y.S. Song, J. Fluoresc. 14 (2004) 289.
[9] G.A. Crosby, J. Chem. Phys. 34 (1961) 743.
[10] M.L. Bhaumid, L.J. Nugent, J. Chem. Phys. 43 (1965) 1680.
[11] A.A. Lamola, G.S. Hamond, J. Chem. Phys. 43 (1965) 2129.
[12] Y. Matsuda, Bull. Chem. Soc. Jpn. 42 (1968) 1513.
[13] J.J. Milkula, J. Chem. Phys. 45 (1966) 2140.
[14] H.J. Zhang, B. Yan, S.B. Wang, J.Z. Ni, J. Photochem. Photobiol. A Chem. 109 (1997) 223.
[15] B. Yan, H.J. Zhang, S.B. Wang, J.Z. Ni, Spectrosc. Lett. 31 (1998) 603.
[16] B. Yan, H.J. Zhang, S.B. Wang, J.Z. Ni, Monatsh. Chem. 129 (1998) 151.
[17] B. Yan, H.J. Zhang, S.B. Wang, J.Z. Ni, Monatsh. Chem. 129 (1998) 567.
[18] B. Yan, H.J. Zhang, S.B. Wang, J.Z. Ni, Chem. Pap. 52 (1998) 199.
[19] B. Yan, H.J. Zhang, S.B. Wang, J.Z. Ni, J. Chin. Chem. Soc. 44 (1997) 567.
[20] B. Yan, H.J. Zhang, S.B. Wang, J.Z. Ni, J. Photochem. Photobiol. A Chem. 116 (1998) 209.
[21] B. Li, H.J. Zhang, J.F. Ma, S.B. Wang, J.Z. Ni, Chin. Sci. Bull. 42 (1996) 825.
[22] H.J. Zhang, B. Li, J.F. Ma, J.Z. Ni, Thin Solid Films 310 (1997) 274.

[23] S. Sato, M. Wada, Bull. Chem. Soc. Jpn. 43 (1970) 1955.
[24] B. Yan, H.J. Zhang, J.Z. Ni, Chin. J. Mol. Sci. 15 (1997) 20.
[25] B. Yan, H. Shao, H.J. Zhang, S.B. Wang, J.Z. Ni, Chin. J. Inorg. Chem. 14 (1998) 407.
[26] B. Yan, H.J. Zhang, J.Z. Ni, Chem. Res. Chin. Univ. 14 (1998) 245.
[27] D.L. Dexter, J. Chem. Phys. 21 (1953) 836.
[28] C.R.S. Dean, T.M. Shepherd, J. Chem. Soc., Faraday Trans. II 71 (1975) 146.